SUPPORTING INFORMATION

Air-stable and Reusable Cobalt Phosphide Nanoalloy Catalyst for Selective Hydrogenation of Furfural Derivatives

Hiroya Ishikawa,[a] Min Sheng,[a] Ayako Nakata,[b] Kiyotaka Nakajima,[c] Seiji Yamazoe,[d] Jun Yamasaki,[e] Sho Yamaguchi,[a] Tomoo Mizugaki,[a] and Takato Mitsudome*[a]*

*E-mail for T. Mit.: mitsudom@cheng.es.osaka-u.ac.jp.
*E-mail for A. N.: NAKATA.ayako@nims.go.jp

[a]Department of Materials Engineering Science, Graduate School of Engineering Science, Osaka University, 1-3 Machikaneyama, Toyonaka, Osaka 560-8531, Japan
[b]First-Principles Simulation Group, Nano-Theory Field, International Center for Materials Nanoarchitectonics (WPI-MANA), National Institute for Materials Science (NIMS), 1-1 Namiki, Tsukuba, Ibaraki 305-0044, Japan
[c]Institute for Catalysis, Hokkaido University, Kita 21 Nishi 10, Kita-ku, Sapporo 001-0021, Japan
[d]Department of Chemistry, Tokyo Metropolitan University, 1-1 Minami Osawa, Hachioji, Tokyo 192-0397, Japan
[e]Research Center for Ultra-High Voltage Electron Microscopy, Osaka University, 7-1, Mihogaoka, Ibaraki, Osaka 567-0047, Japan

Table of Contents

1. General experimental details

All precursors and solvents were used as received, without further purification. $CoCl_2 \cdot 6H_2O$, and 1-octadecene (technical grade 90%) were purchased from the Nacalai Tesque, INC. and Sigma-Aldrich, respectively. Hexadecylamine and triphenyl phosphite were purchased from Tokyo Chemical Industry Co., Ltd. Acetone, chloroform, *n*-hexane, methanol, 2-propanol, 1,4-dioxane, and NaOH were purchased from FUJIFILM Wako Pure Chemical Corporation. Al_2O_3 was obtained from Sumitomo Chemical Co., Ltd. Hydroxyapatite was purchased from FUJIFILM Wako Pure Chemical Corporation. ZrO_2 (JRC ZRO-8) and MgO (JRC-MGO-3 1000A) were provided by the Catalysis Society of Japan as reference catalysts. Bulk Co_2P was purchased from Mitsuwa Chemicals. 5-Hydroxymethylfurfural (HMF) was purchased from FUJIFILM Wako Pure Chemical Corporation. Furfural, 5-methylfurfural and 5-acetoxymethylfurfural were purchased from Tokyo Chemical Industry Co., Ltd. HMF and 5-acetoxymethylfurfural were used as received, without further purification. Furfural and 5-methylfurfural were purified by distillation before use.

Inductively coupled plasma-atomic emission spectroscopy (ICP-AES) was performed using a Perkin Elmer Optima 8300 instrument. ^{1}H and ^{13}C nuclear magnetic resonance (NMR) spectra were recorded using a JEOL JNM-ESC400 spectrometer and chemical shifts (δ) are reported in ppm relative to tetramethylsilane. Transmission electron microscopy (TEM) observations were carried out using a FEI Tecnai G2 20ST instrument operated at 200 kV. Scanning transmission electron microscopy (STEM) images with elemental maps were collected using a FEI Titan Cubed G2 60-300 instrument operated at 300 kV and equipped with Super-X energy-dispersive X-ray spectroscopy (EDX) detector. Elemental mapping based on quantification analysis of EDX spectra was carried out using Esprit. Co *K*-edge X-ray absorption spectra were recorded at room temperature at the BL01B1 and BL14B2 lines, using a Si (111) monochromator at SPring-8, Japan Synchrotron Radiation Research Institute (JASRI), Harima, Japan. Data analysis was performed using the xTunes software [S1]. XRD (X-ray diffraction) studies were conducted on a Philips X′Pert-MPD diffractometer with Cu-Kα radiation (45 kV, 40 mA). Fourier-transform infrared (FT-IR) spectra were recorded using a JASCO FT-IR 4100 spectrometer equipped with a mercury cadmium telluride detector at a spectral resolution of 4 cm^{-1} with 128 scans accumulated. A thin disk was prepared by pressing the sample powder (pure nano-Co_2P/Al_2O_3 or 3 wt% nano-Co_2P in KBr) onto a stainless-steel grid. The sample disk was then placed inside an IR cell with CaF_2 windows to enable thermal treatment in a controlled atmosphere. The sample pellet was treated under vacuum (< 1 mmHg) at 130 °C for 1 h, after which the probe molecule was introduced to the sample disk and evacuated at room temperature. X-ray photoelectron spectroscopy (XPS) analysis was performed on a Kratos AXIS 165 X-ray photoelectron spectrometer equipped with a monochromatic Al X-ray source. The spectra were obtained at a pass energy of 80.0 eV with an

Al Kα X-ray source operating at 12 mA and 15 kV. The working pressure in the analysis chamber was less than 5.0×10^{-9} mmHg. The C 1s peak at a binding energy of 284.5 eV was used as the internal reference.

2. Characterization

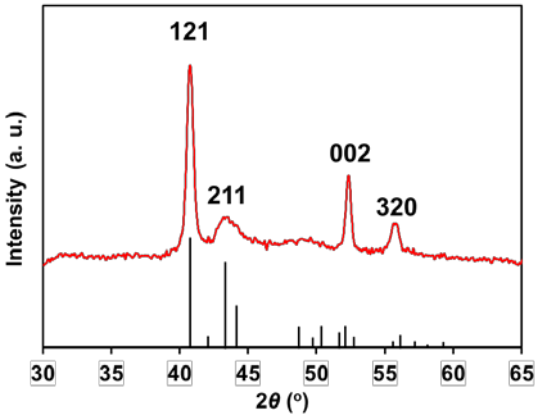

Figure S1. XRD spectrum of nano-Co_2P. The reference pattern of Co_2P is from references S2 and S3 (JCPDS No. 32-0306).

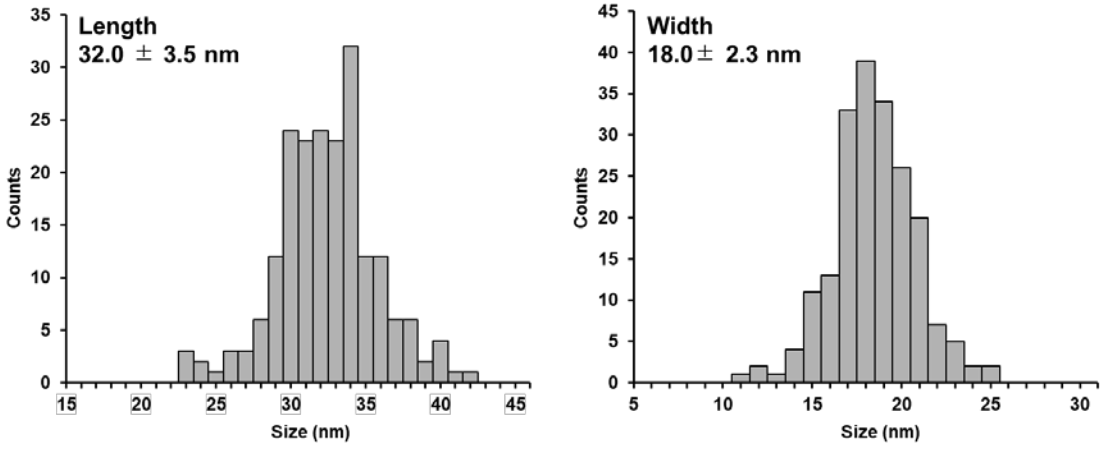

Figure S2. Size distribution histograms (length and width) of the nano-Co_2P.

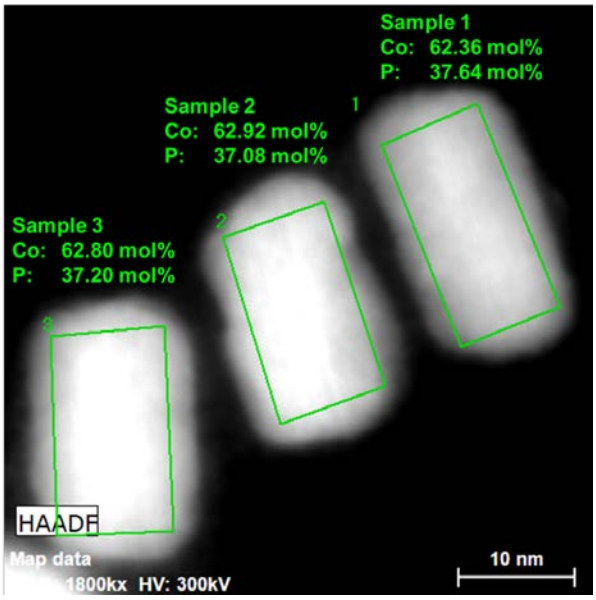

Figure S3. EDX analysis of nano-Co_2P in the green squares.

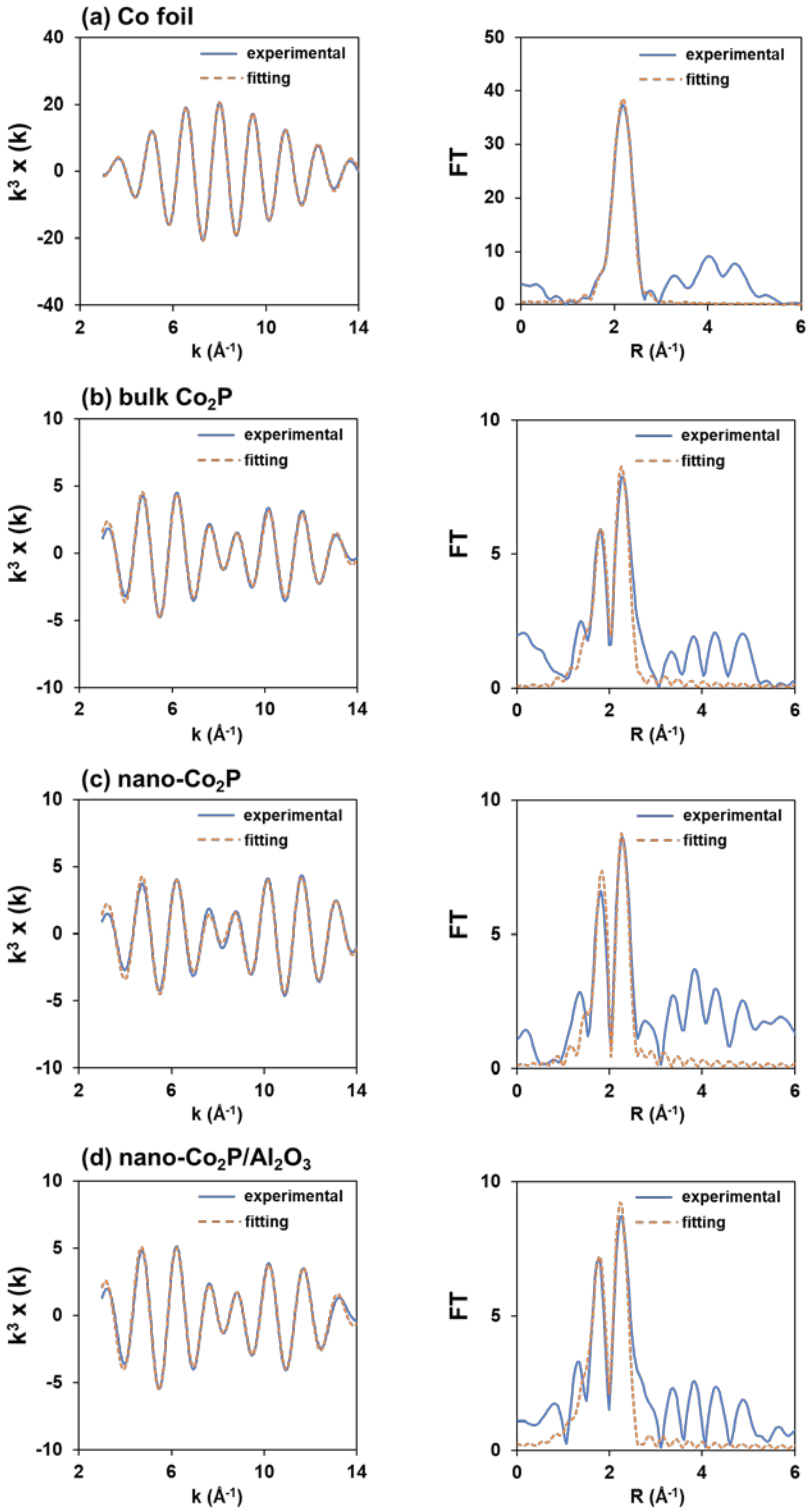

Figure S4. EXAFS fitting curves in k-space (left panel) and R-space (right panel) of (a) Co foil, (b) bulk Co_2P, (c) nano-Co_2P, and (d) nano-Co_2P/Al_2O_3.

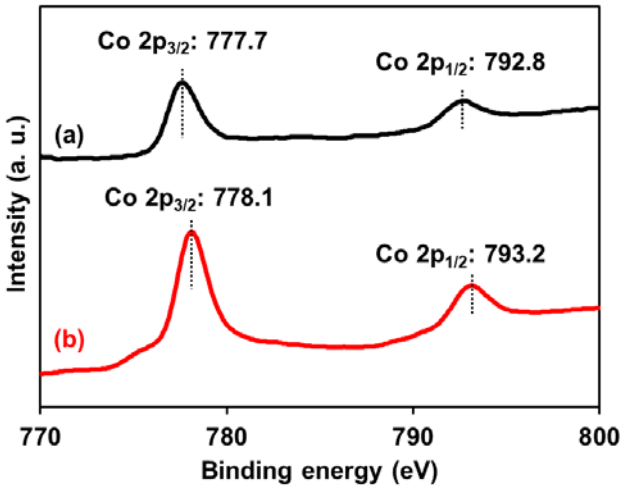

Figure S5. Co 2p XPS spectra of (a) nano-Co_2P and (b) nano-Co_2P/Al_2O_3.

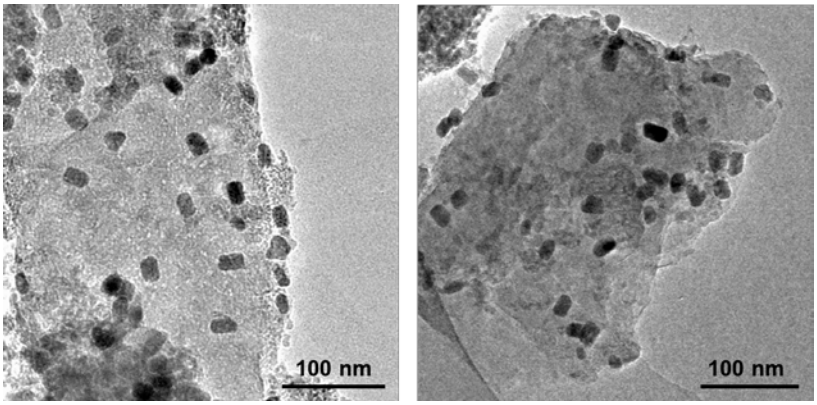

Figure S6. TEM images of nano-Co_2P/Al_2O_3 before (left) and after reaction (right).

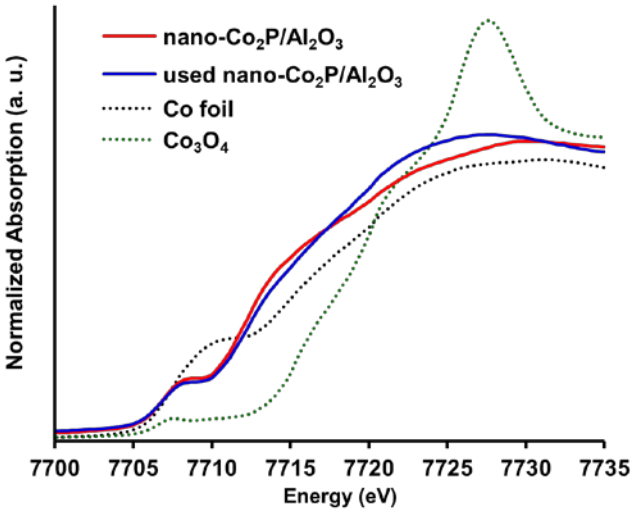

Figure S7. Co *K*-edge XANES spectra of nano-Co_2P/Al_2O_3 and used nano-Co_2P/Al_2O_3 with Co foil and Co_3O_4 as references.

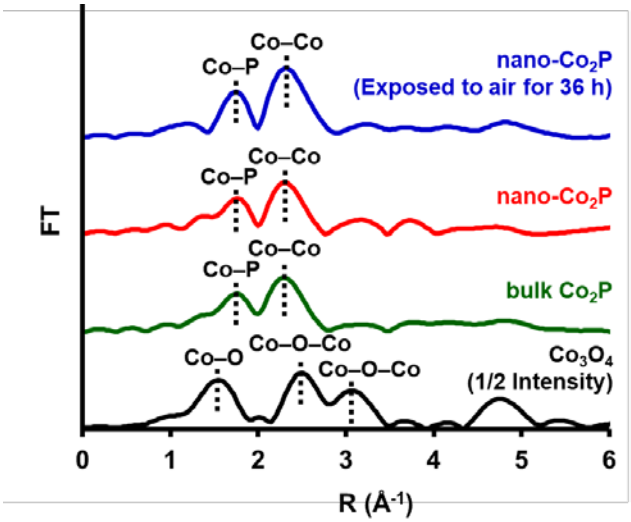

Figure S8. Fourier transforms of the k^3-weighted EXAFS spectra of nano-Co_2P and nano-Co_2P exposed to air with bulk Co_2P and Co_3O_4 as references.

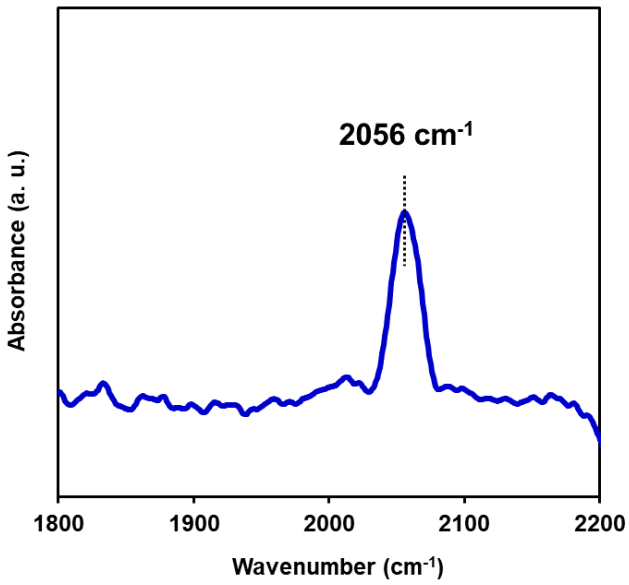

Figure S9. FT-IR spectrum of CO adsorbed on nano-Co_2P.

Table S1. Curve-fitting results of Co *K*-edge EXAFS for Co foil, bulk Co_2P, nano-Co_2P, and nano-Co_2P/Al_2O_3.

sample	shell	*CN*[a]	*r* (Å)[b]	D.W.[c]	R factor (%)
Co foil	Co–Co	10.6±0.2	2.49±0.01	0.007±0.002	2.6
bulk Co_2P	Co–P	2.0±0.1	2.24±0.03	0.005±0.002	9.4
	Co–Co	4.0±0.2	2.56±0.02	0.010±0.003	
nano-Co_2P	Co–P	1.8±0.1	2.23±0.02	0.003±0.002	12.5
	Co–Co	3.5±0.2	2.56±0.02	0.009±0.003	
nano-Co_2P/Al_2O_3	Co–P	2.1±0.2	2.20±0.03	0.005±0.003	10.3
	Co–Co	3.3±0.2	2.56±0.02	0.009±0.004	

[a]Coordination number. [b]Bond distance. [c]Debye–Waller factor.

Table S2. The elemental analysis of fresh and used nano-Co_2P/Al_2O_3 by ICP-AES.

	wt%	
	Co	P
nano-Co_2P/Al_2O_3	1.96	0.68
used nano-Co_2P/Al_2O_3	2.04	0.74

3. Hot filtration experiment

Scheme S1. Hot filtration experiment of nano-Co_2P/Al_2O_3 in hydrogenation of HMF to BHMF.

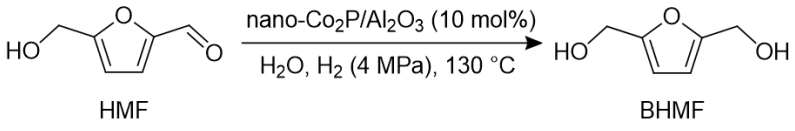

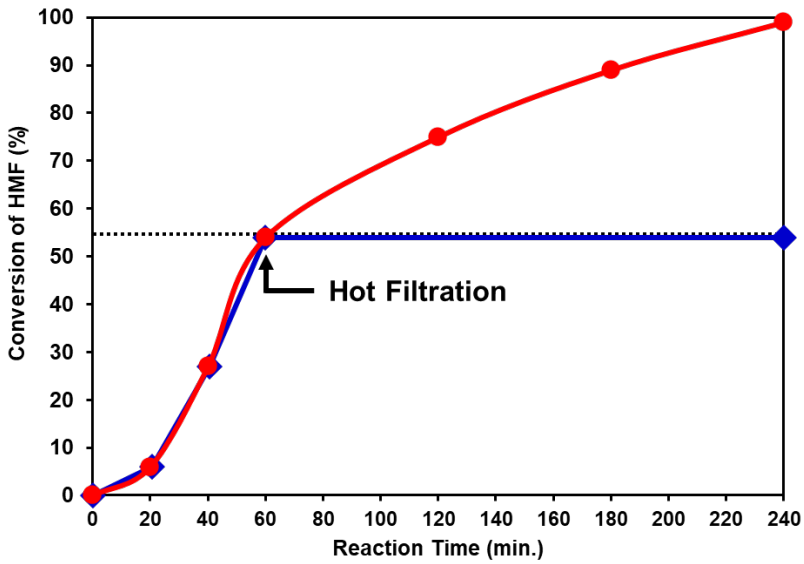

Reaction conditions: nano-Co_2P/Al_2O_3 (75 mg), HMF (0.25 mmol), water (3 mL), H_2 (4 MPa), 130 °C. Conversion was determined by GC-MS using an internal standard technique. Red spheres (●): Without filtration of the catalyst. Blue diamonds(♦): With removal of the catalyst by hot filtration after 1 h.

4. Effect of solvent

Table S3. Effect of reaction solvents on the hydrogenation of furfural derivatives using nano-Co_2P/Al_2O_3.[a]

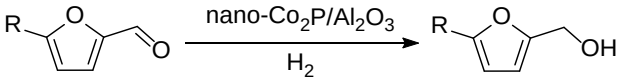

entry	substrate	solvent	conv.[b] (%)	sel.[b] (%)
1	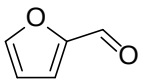	H_2O	76	71
2		MeOH	85	99
3		1,4-dioxane	29	93
4	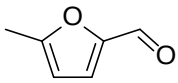	H_2O	90	77
5		MeOH	91	99
6		1,4-dioxane	36	92
7[c]	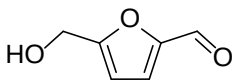	H_2O	54	>99
8[c]		MeOH	31	89
9[c]		1,4-dioxane	5	80
10[d]	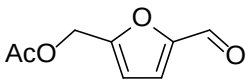	H_2O	>99[e]	<1[e,f]
11[d]		MeOH	>99[e]	<1 [e,f]
12[d]		1,4-dioxane	>99[e]	82[e]

[a]Reaction conditions: nano-Co_2P/Al_2O_3 (6.7 mol%), substrate (0.25 mmol), solvent (3 mL), H_2 (4 MPa), 130 °C, 2 h. [b]Determined by GC-MS using an internal standard technique. [c]nano-Co_2P/Al_2O_3 (10 mol%), 1 h. [d]H_2 (5 MPa), 150 °C, 12 h. [e]Determined by ^{1}H NMR using an internal standard technique. [f]BHMF was detected as the main product.

5. DFT calculation

Computational details

Density functional theory (DFT) calculations were performed using the CONQUEST program [S4, S5]. The Perdew, Burke and Ernzerhof (PBE) exchange-correlation functional [S6] was used with a norm-conserving pseudopotential and real-space pseudo atomic orbital (PAO) basis functions [S7]. We used the double-zeta plus polarization (DZP) type PAOs. The ranges of two s, two d and a p PAOs for Co were {(7.8, 6.1), (4.5, 2.1) and (7.8)} bohr, those of two s, two p and a d PAOs for P, C, N and O were {(5.2, 4.0), (6.5, 4.6) and (6.5)}, {(4.6, 3.4), (5.7, 3.7) and (5.7)}, {(4.1, 2.9), (5.0, 3.1) and (5.0)} and {(3.7, 2.5), (4.6, 2.6) and (4.6)} bohr, and those of two s and a p PAOs for H were {(5.5, 4.0) and (5.5)}. The basis set superposition errors (BSSEs) were corrected by the counterpoise method [S8]. The dispersion energies were considered by using the DFT-D2 method [S9].

As shown in Figure S10, the unit cell of Co_2P consists of two layers, six Co atoms in the pyramidal site (P-site) and two P atoms in the first layer and six Co atoms in the tetrahedral site (T-site) and four P atoms in the second layer [S10]. The periodic boundary condition with 8×8×1 grid was used for the surface system. For the surface calculation, we used a supercell slab consisting of eight layers (about 12 Å thickness) with a vacuum gap (about 15 Å). A cis-furfural molecule was put on Co_2P (0001) surface with the width of 11.5×10.0 $Å^2$.

Adsorption of furfural to Co_2P (0001) surface

There are many possible adsorption sites of furfural to the Co_2P (0001) T-site surface. The optimized structures of furfural at the sites are shown in Figure S11. The structures t1_h-b, t3_b-o and t2_h-b(2) are shown as the representatives of groups A, B and C in the manuscript because their adsorption energies are the closest to the mean adsorption energy of the groups. The adsorption energies, $\Delta E = E(Co_2P\text{-furfural}) - E(Co_2P) - E(\text{furfural})$ are summarized in Table S4. The bond lengths of isolated furfural and their changes by the adsorption are given in Table S5. The change of the electron distribution before and after the adsorption were investigated by Mulliken population analysis [S11].

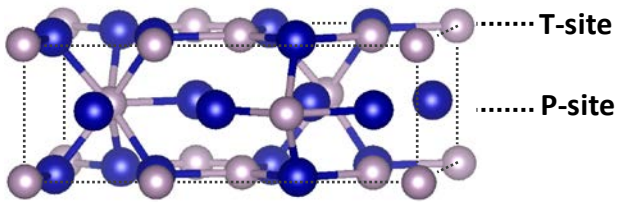

Figure S10. Unit cell of Co_2P.

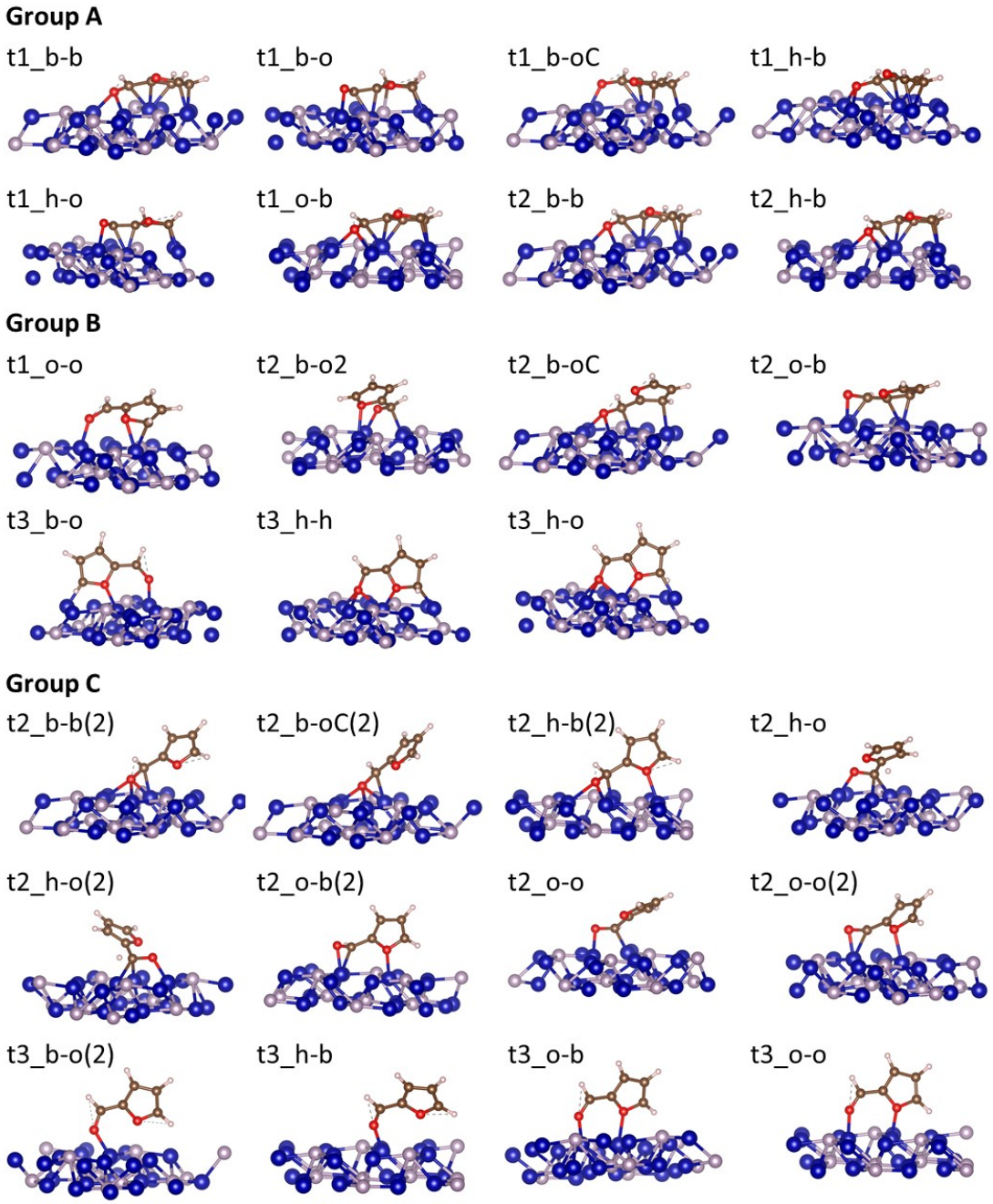

Figure S11. Optimized structures of furfural molecule adsorbed to Co_2P (0001) surface. Groups A, B and C are the structures in which both the C=O bond and the furan ring were adsorbed parallelly to the surface, O in C=O and a C-O bond in the furan ring were adsorbed to the surface, and only C=O was strongly adsorbed to the surface, respectively. The labels "x_y-z" corresponds to the initial structure: x corresponds to the adsorption parallelly (t1), diagonally (t2) and perpendicularly (t3) to the surface, y and z correspond to the position of O atoms in CHO and furan ring, o = on-top, b = bridge, h = hollow sites of Co triangle. oC means C atom in CHO is on-top of Co atom.

Table S4. Adsorption energy of furfural to Co_2P (0001) surface (kcal/mol) The labels of the adsorption structure correspond to those in Figure S11.

	Adsoprtion structure								Mean value
Group A	t1_b-b	t1_b-o	t1_b-oC	t1_h-b	t1_h-o	t1_o-b	t2_b-b	t2_h-b	
	-76.1	-48.0	-57.5	-74.8	-57.6	-76.1	-75.4	-75.8	-67.7
Group B	t1_o-o	t2_b-o	t2_b-oC	t2_o-b	t3_b-o	t3_h-h	t3_h-o		
	-37.4	-40.2	-50.2	-52.7	-41.9	-36.9	-37.7		-42.4
Group C	t2_b-b (2)	t2_b-oC(2)	t2_h-b(2)	t2_h-o	t2_h-o(2)	t2_o-b(2)	t2_o-o	t2_o-o(2)	
	-36.6	-37.0	-35.6	-38.5	-38.5	-27.3	-30.9	-27.5	-32.2
	t3_b-o(2)	t3_h-b	t3_o-b	t3_o-o					
	-26.0	-27.5	-31.1	-30.4					

Table S5. Bond lengths of the isolated furfural molecule and the bond-length differences from the isolated molecule for the adsorption structures in groups A, B, and C (Å). The labels of the adsorption structure correspond to those in Figure S11.

		Adsoprtion structure								Mean value
		isolated molecule								
C=O	C=O	1.234								
	C-C (1)	1.469								
Furan	C-O	1.379								
	O-C	1.362								
	C=C (1)	1.392								
	C-C (2)	1.433								
	C=C (2)	1.399								
Group A		t1_b-b	t1_b-o	t1_b-oC	t1_h-b	t1_h-o	t1_o-b	t2_b-b	t2_h-b	
C=O	C=O	0.137	0.097	0.087	0.138	0.098	0.136	0.139	0.138	0.121
	C-C (1)	-0.022	0.010	-0.026	-0.021	-0.011	-0.024	-0.022	-0.025	-0.018
Furan	C-O	-0.002	0.009	0.020	-0.002	0.017	-0.002	-0.001	-0.002	0.005
	O-C	0.054	0.112	0.097	0.058	0.073	0.054	0.055	0.056	0.070
	C=C (1)	0.043	0.101	0.125	0.042	0.087	0.047	0.048	0.046	0.067
	C-C (2)	0.068	0.098	0.043	0.068	0.099	0.066	0.066	0.063	0.071
	C=C (2)	0.081	0.114	0.053	0.081	0.125	0.077	0.081	0.076	0.086
Group B		t1_o-o	t2_b-o2	t2_b-oC	t2_o-b	t3_b-o	t3_h-h	t3_h-o		
CHO	C=O	0.061	0.119	0.171	0.071	0.055	0.140	0.108		0.104
	C-C (1)	-0.052	0.008	0.019	0.009	-0.043	-0.076	-0.063		-0.028
Furan	C-O	0.027	0.024	-0.011	0.036	0.017	0.017	0.028		0.020
	O-C	0.090	0.034	0.019	0.015	0.087	0.105	0.063		0.059
	C=C (1)	0.074	-0.009	-0.013	-0.007	0.044	0.095	0.056		0.034
	C-C (2)	-0.037	0.005	0.031	0.037	-0.024	-0.045	-0.027		-0.009
	C=C (2)	0.035	-0.001	0.041	0.056	0.019	0.048	0.031		0.033
Group C		t2_b-b (2)	t2_b-oC(2)	t2_h-b(2)	t2_h-o	t2_h-o(2)	t2_o-b(2)	t2_o-o	t2_o-o(2)	
CHO	C=O	0.142	0.140	0.170	0.111	0.114	0.090	0.098	0.089	0.093
	C-C (1)	-0.002	-0.004	0.020	0.024	0.028	0.029	0.005	0.012	-0.001
Furan	C-O	0.008	-0.006	0.025	0.012	0.021	0.027	0.001	0.023	0.014
	O-C	0.017	0.008	0.021	0.011	0.014	0.036	0.014	0.036	0.019
	C=C (1)	-0.007	-0.003	-0.012	-0.001	-0.002	-0.013	-0.002	-0.011	-0.004
	C-C (2)	0.006	0.005	0.008	0.002	0.004	0.013	0.002	0.009	0.002
	C=C (2)	0.000	0.004	-0.005	0.006	-0.002	-0.014	0.003	-0.012	0.001
		t3_b-o(2)	t3_h-b	t3_o-b	t3_o-o					
CHO	C=O	0.048	0.038	0.040	0.036					
	C-C (1)	-0.032	-0.032	-0.032	-0.031					
Furan	C-O	0.006	0.012	0.022	0.020					
	O-C	0.006	0.015	0.025	0.026					
	C=C (1)	0.004	0.000	-0.001	-0.004					
	C-C (2)	-0.005	-0.005	-0.007	-0.006					
	C=C (2)	0.009	0.007	0.008	0.007					

Table S6. Electronic charge differences of furan and CHO in adsorbed furfural molecules from isolated furfural molecules. Changes of O atoms are also given. Negative value means that the base gets electrons. The labels of the adsorption structure correspond to those in Figure S11.

	Adsoprtion structure								Mean value
Group A	t1_b-b	t1_b-o	t1_b-oC	t1_h-b	t1_h-o	t1_o-b	t2_b-b	t2_h-b	
furan	-0.06	0.08	0.00	-0.07	0.09	-0.06	-0.06	-0.06	-0.02
O in furan	-0.07	-0.10	-0.13	-0.07	-0.09	-0.07	-0.07	-0.07	-0.08
CHO	-0.10	-0.08	-0.05	-0.09	-0.10	-0.10	-0.10	-0.10	-0.09
O in CHO	-0.19	-0.11	-0.10	-0.19	-0.11	-0.19	-0.19	-0.19	-0.16
total	-0.16	0.00	-0.05	-0.16	-0.01	-0.16	-0.16	-0.16	-0.11
Group B	t1_o-o	t2_b-o2	t2_b-oC	t2_o-b	t3_b-o	t3_h-h	t3_h-o		
furan	-0.13	-0.07	0.00	-0.05	-0.12	-0.14	-0.10		-0.09
O in furan	-0.12	0.01	-0.01	0.01	-0.06	-0.06	-0.05		-0.04
CHO	-0.05	-0.11	-0.21	-0.09	-0.03	-0.23	-0.18		-0.13
O in CHO	0.01	-0.02	-0.07	-0.05	0.03	-0.13	-0.07		-0.04
total	-0.11	-0.01	-0.08	-0.03	-0.03	-0.18	-0.12		-0.08
Group C	t2_b-b2	t2_b-oC2	t2_h-b2	t2_h-o	t2_h-o2	t2_o-b2	t2_o-o	t2_o-o2	
furan	-0.03	0.01	-0.05	-0.03	-0.04	-0.08	-0.02	-0.07	-0.04
O in furan	-0.02	0.01	-0.02	0.00	0.00	-0.05	0.02	-0.01	0.00
CHO	-0.21	-0.22	-0.20	-0.11	-0.11	-0.09	-0.12	-0.09	-0.10
O in CHO	-0.04	-0.05	-0.05	-0.05	-0.05	-0.05	-0.05	-0.06	-0.01
total	-0.06	-0.04	-0.08	-0.05	-0.05	-0.10	-0.03	-0.07	-0.01
	t3_b-o2	t3_h-b	t3_o-b	t3_o-o					
furan	-0.01	-0.03	-0.05	-0.05					
O in furan	0.00	0.04	0.01	0.00					
CHO	-0.03	0.00	0.00	0.02					
O in CHO	0.06	0.07	0.06	0.07					
total	0.06	0.12	0.07	0.07					

6. Product identification

Table 1 and Scheme 2

Bis(2,5-hydroxymethyl)furan (BHMF) [S12]

CAS registry No. [1883-75-6]. ^{1}H NMR (DMSO, 400 MHz): δ = 6.18 (s, 2H), 5.13 (t, *J* = 5.7 Hz, 2H), 4.35 (d, *J* = 6.0 Hz, 4H). ^{13}C NMR (DMSO, 100 MHz): δ = 154.7, 107.3, 55.7.

Scheme 1(a)

Furfuryl alcohol [S13]

CAS registry No. [98-00-0]. ^{1}H NMR ($CDCl_3$, 400 MHz): δ = 7.40 (d, *J* = 1.5 Hz, 1H), 6.35–6.33

(m, 1H), 6.29 (d, *J* = 3.2 Hz, 1H), 4.61 (s, 2H), 1.79 (brs, 1H). ^{13}C NMR ($CDCl_3$, 100 MHz): δ = 154.0, 142.7, 110.3, 107.7, 57.5.

Scheme 1 (b)

5-Methylfurfuryl alcohol [S14]

CAS registry No. [3857-25-8]. ^{1}H NMR ($CDCl_3$, 400 MHz): δ = 6.16 (d, *J* = 2.8 Hz, 1H) , 5.91–5.90 (m, 1H), 4.54 (s, 2H), 2.29 (s, 3H). ^{13}C NMR ($CDCl_3$, 100 MHz): δ = 152.4, 152.3, 108.7, 106.2, 57.5, 13.5.

Scheme 1 (c)

2,5-Furandimethanol monoacetate [S15]

CAS registry No. [89630-82-0]. ^{1}H NMR ($CDCl_3$, 400 MHz): δ = 6.35 (d, *J* = 3.4 Hz, 1H), 6.26 (d, *J* = 2.7 Hz, 1H) , 5.03 (s, 2H), 4.63 (s, 2H), 2.08 (s, 3H). ^{13}C NMR ($CDCl_3$, 100 MHz): δ = 170.6, 154.8, 149.5, 111.4, 108.5, 58.1, 57.5, 20.8.

References

S1. Asakura, H.; Yamazoe, S.; Misumi, T.; Fujita, A.; Tsukuda, T.; Tanaka, T. xTunes: A New XAS Processing Tool for Detailed and on-the-fly Analysis. *Rad. Phys. Chem.* **2020**, *175*, 108270.

S2. Pradhan, B.; Kumar, G. S.; Dalui, A.; Khan, A. H.; Satapati, B.; Ji, Q.; Shrestha, L. K.; Aruga, K.; Acharya, S. Shape-Controlled Cobalt Phosphide Nanoparticles as Volatile Organic Solvent Sensor. *J. Mater. Chem. C* **2016**, *4*, 4967–4977.

S3. Ni, Y.; Li, J.; Zhang, L.; Yang, S.; Wei, X. Urchin-like Co_2P Nanocrystals: Synthesis, Characterization, Influencing Factors and Photocatalytic Degradation Property. *Mater. Res Bull.* **2009**, *44*, 1166–1172.

S4. Conquest website, http://www.order-n.org, (accessed April 2020).

S5. Nakata, A.; Baker, J.; Mujahed, S.; Poulton, J. T. L.; Arapan, S.; Lin, J.; Raza, Z.; Yadav, S.; Truandier, L.; Miyazaki, T.; Bowler, D. R. Large Scale and Linear Scaling DFT with the CONQUEST Code. *J. Chem. Phys*. **2020**, *152*, 164112.

S6. Perdew, J. P.; Burke, K.; Ernzerhof, M. Generalized Gradient Approximation Made Simple. *Phys. Rev. Lett.* **1996**, *77*, 3865–3868.

S7. Torralba, A. S.; Todorović, M.; Brázdová, V.; Choudhury, R.; Miyazaki, T.; Gillan, M. J.; Bowler, D. R. Pseudo-Atomic Orbitals as Basis Sets for the O(N) DFT Code CONQUEST. *J. Phys.: Condens. Matter* **2008**, *20*, 294206.

S8. van Duijneveldt, F. B.; van Duijneveldt-van de Rijdt, J. G.; van Lenthe, J. H. State of the Art

in Counterpoise Theory. *Chem. Rev.* **1994**, *94*, 1873−1885.

S9. Grimme, S. Semiempirical GGA-Type Density Functional Constructed with a Long-Range Dispersion Correction. *J. Comp. Chem*. **2006**, *27*, 1787–1799.

S10. Mitsudome, T.; Sheng, M.; Nakata, A.; Yamasaki, J.; Mizugaki, T.; Jitsukawa, K. A Cobalt Phosphide Catalyst for the Hydrogenation of Nitriles. *Chem. Sci*. **2020**, *11*, 6682–6689.

S11. Mulliken, R. S. Electronic Population Analysis on LCAO–MO Molecular Wave Functions. I. *J. Chem. Phys.* **1955**, *23*, 1833–1840.

S12. Watari, R.; Matsumoto, N.; Kuwata, S.; Kayaki, Y. Distinct Promotive Effects of 1,8-Diazabicyclo[5.4.0]undec-7-ene (DBU) on Polymer Supports in Copper-Catalyzed Hydrogenation of C=O Bonds. *ChemCatChem* **2017**, *9*, 4501–4507.

S13. Tamura, M.; Tokonami, K.; Nakagawa, Y.; Tomishige, K. Rapid Synthesis of Unsaturated Alcohols under Mild Conditions by Highly Selective Hydrogenation. *Chem. Commun*. **2013**, *49*, 7034–7036.

S14. Jung, M. E.; Im, G. J. Total Synthesis of Racemic Laurenditerpenol, an HIF-1 Inhibitor. *J. Org. Chem.* **2009**, *74*, 8739–8753.

S15. Fotso, S.; Maskey, R. P.; Schröder, D.; Ferrer, A. S.; Grün-Wollny, I.; Laatsch, H. Furan Oligomers and *β*-Carbolines from Terrestrial Streptomycetes. *J. Nat. Prod*. **2008**, *71*, 1630–1633.